PROCEEDINGS OF SCIENCE

X-ray Spectroscopic Study of the ADC Source X1822-371

R. Iaria[a], N. R. Robba*[a], A. DAı´ [a], T. Di Salvo[a], L. Burderi[b], A. Papitto[b], A. Riggio[b,c] and T. Mineo[d]

[a] *DSFA-Universita' degli Studi di Palermo, via Archirafi 36 - 90123 Palermo, Italy*

[b] *Dipartimento di Fisica, Università degli Studi di Cagliari, SP Monserrato-Sestu, KM 0.7, Monserrato, 09042 Italy*

[c] *Osservatorio Astronomico di Cagliari, Poggio dei Pini, Strada 54, 09012 Capoterra (CA), Italy*

[d] *INAF, Istituto di Astrofisica Spaziale e Fisica cosmica di Palermo, via U. La Malfa 153, I-90146 Palermo, Italy*

E-mail: iaria@fisica.unipa.it

We analyse two Chandra HETGS (High Energy Transmission Grating Spectrometer) observations and one XMM-Newton observation. The HETGS and XMM/Epic-pn observed X 1822-371 for 140 and 50 ks, respectively. We extracted an averaged spectrum and five spectra from five selected orbital-phase intervals that are 0.04-0.25, 0.25-0.50, 0.50-0.75, 0.95-1.04; the orbital phase zero corresponds to the eclipse time. The spectra cover the energy band between 0.4 and 12 keV. We confirm the presence of local neutral matter that partially covers the X-ray emitting region; the equivalent hydrogen column is 3.5×10^{22} cm^{-2} and the covered fraction is around 60 %. We detected and identified several emission lines associated with He-like and H-like ions. The He-like transitions of O VII, Ne IX, Mg XI, Si XIII show that the intercombination dominates over the forbidden and resonance lines. The fluxes of the lines are higher during the orbital-phase interval 0.04-0.75 while their intensities decrease during the dip and the eclipse.We discuss the presence of an optically thin corona with optical depth of 0.01 that scatters the luminosity from the inner region indetyfing it with the hot corona showed by [12] in the disc illuminated by a central sources.

8th INTEGRAL Workshop 'The Restless Gamma-ray Universe'- Integral2010, September 27-30, 2010
Dublin Ireland

*Speaker.

PoS(INTEGRAL 2010)138

1. Introduction

X1822-371 is a compact binary system with a period of 5.57 hr. The light curve of the source shows an almost sinusoidal modulation and eclipse. Analysing RXTE data of X1822-371 [1] detected a pulse period of 0.59 s deriving that the orbit of the system is almost circular with an eccentricity less than 0.03, a mass function of $(2.03 \pm 0.03) \times 10^{-2}$ $M_{\odot}$, and a pulse period derivative of $(-2.85 \pm 0.04) \times 10^{-12}$ s s^{-1} indicating that the neutron star is spinning up. The distance to the X1822-371 is 2.5 kpc ([2]) and the measured luminosity is $\sim 10^{36}$ erg s^{-1} (see e.g., [2, 3]), however [1] using the relation between luminosity and spin-up rate found that if X1822-371 is at a luminosity of 10^{36} erg s^{-1} the neutron star magnetic field B should have an unlikely intensity of $\sim 8 \times 10^{16}$ G while for a luminosity of 10^{38} erg s^{-1} $B \sim 8 \times 10^{10}$ G. [4] using ultraviolet and visual data of X1822-371 well constrained the inclination angle i of the source at $82.5^{\circ} \pm 1.5^{\circ}$, this value indicates that the modulation in the light curve of X1822-371 cannot be due to dips because these can be observed for inclination angles between 60° and 80° ([5]). [6] analysed the eclipse arrival times of X1822-371 using data from RXTE, XMM-Newton, and Chandra observations, spanning the years from 1996 to 2008. Combining these eclipse arrival time measurements with those already available ([7] and reference therein) covering from 1977 to 1996, the authors found that the orbital period of the binary system increases with a rate $\dot{P}_{\rm orb} = 1.499(71) \times 10^{-10}$ s/s, that is three orders of magnitude larger than what is expected from conservative mass transfer driven by magnetic braking and gravitational radiation. [6] concluded that the mass transfer rate from the companion star is between 3.5 and 7.5 times the Eddington limit suggesting that the mass transfer has to be highly non-conservative with the neutron star accreting at the Eddington limit and the rest of the transferred mass expelled from the system. [8] studying the optical and UV data of X1822-371 reached similar results.

The eclipse observed in the X-ray light curve of X1822-371 is partial, this argument combined with the high inclination angle of the system suggests that we observe the X-ray emission coming from an extended corona above the disc, the so-called accretion disc corona (ADC, [9]). The properties of the ADC are still debated. In a scenario with an optically thin ADC we should expect that only a small part of the emission produced in the inner region is scattered by the ADC along the line of sight (see e.g. [10]), on the other hand an optically thick corona should imply that it is itself seat of the observed extended emission ([9]). [11] analysed simultaneous observations with *Rossi X-Ray Timing Explorer* (RXTE) and ASCA of X1822-371. They showed that both the source spectrum and light curve can be well fitted by two equivalent models, representing the scenario in which X1822-371 has an optically thick corona or an optically-thin corona, respectively. Both these models could well describe the data. [3] analysed a BeppoSAX observation of X1822-371 finding that the continuum emission is well fitted using a Comptonised component with an electron temperature of 4.5 keV that is partially covered by a local neutral absorber. The authors suggested that the Comptonised emission is due to a diffuse emission from the ADC while the partial covering is produced by a cold wall subtending an angle of 16° with respect to the equatorial plane and placed in the external edge of the accretion disc.

In this work we briefly present the analysis of two Chandra/HETGS observations and show why the presence of an extended optically thin corona well explains our results.

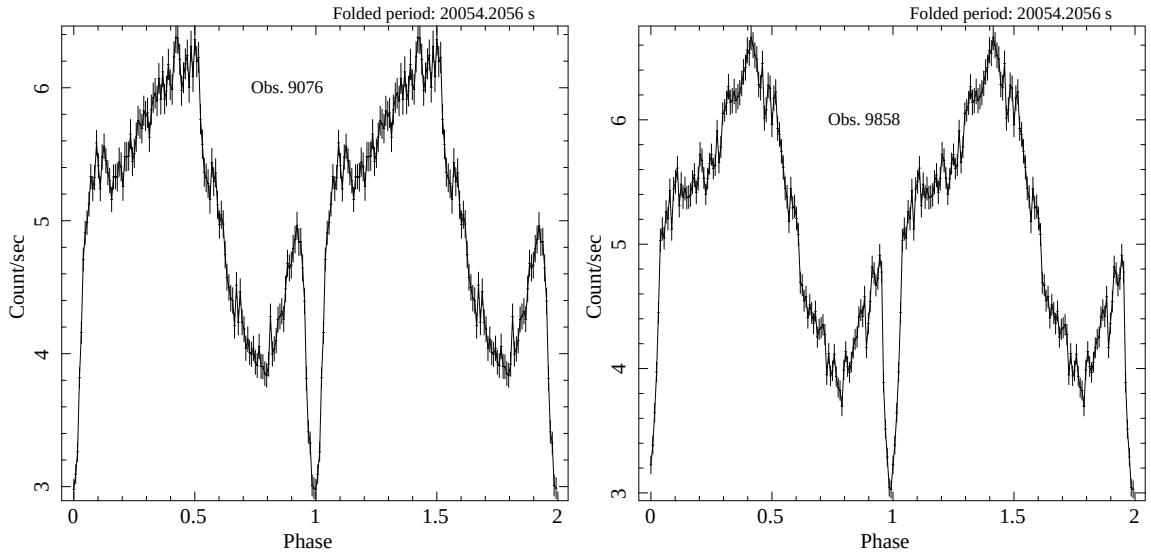

Figure 1: Folded light curves corresponding to the Obs. ID. 9076 and the Obs. ID. 9858. The data were folded adopting the recent ephemeris obtained by [6] and using 128 channels per period.

2. Observation and spectral analysis

X1822-371 was observed with the Chandra observatory using the HETGS for a total observation time of 66 and 84 ks (Obsid. 9076 and 9858), respectively. Both observations were performed in timed faint mode. The region of sky containing X1822-371 was observed by XMM-Newton for a duration of 53.8 ks (Obs. ID. 0111230101). For our analysis we used only the Reflection Grating Spectrometers (RGSs) and Epic-pn data. We summed the first-order HEG (and MEG) spectra of the two Chandra observations to increase the statistics obtaining a total exposure time of 142 ks. The MEG and HEG energy range was 0.5-7 keV and 0.77-10 keV, respectively. We extracted the RGS1, RGS2, and Epic-pn spectra from the whole observation with an exposure time of 43, 42, 38 ks, respectively and adopted a 0.4-2 keV energy range for RGS spectra and 1-12 keV for Epic-pn spectrum. We fitted the continuum emission adopting the model proposed by [3] for the broad band BeppoSAX spectrum of X1822-371: i.e. a Comptonised component (`Compst` in XSPEC) partially absorbed by neutral matter and absorbed by interstellar matter (`wabs` in XSPEC).

Adopting this continuum to fit the RGS and Epic-pn data we found a value of $\chi^2_{\rm red}$(d.o.f.) that was 1.89(2321). Since the residuals showed the presence of several emission lines we added seven Gaussian components associated with the O VII intercombination line, O VIII, Ne IX intercombination line, Si XIV, Fe I, Fe XXV intercombination line, and Fe XXVI respectively. The addition of the Gaussian profiles improved the fit giving a $\Delta\chi^2$ of 1613 and a $\chi^2_{\rm red}$(d.o.f.) of 1.18(2302). Fitting the HETGS spectra with the same model we obtained a value of $\chi^2_{\rm red}(\text{d.o.f.}) = 0.92(3507)$; in the residuals we observe several emission features. To fit the residuals we added ten Gaussian components and identified the emission lines associated with the following transitions: O VII intercombination line, O VIII Lyα, Ne IX intercombination line, Ne X Lyα, Mg XI intercombination line, Mg XII Lyα, Si XIII intercombination line, Si XIV Lyα, Fe I Kα, Fe XXVI Lyα. The addition of the Gaussian components improved the fit with a $\Delta\chi^2$ of 805 and a value of $\chi^2_{\rm red}$(d.o.f.) of

0.68(3478). The best-fitting values of the continuum parameters obtained from HETGS and XMM spectra are compatible with those obtained by [3] and are consistent with each other.

Table 1: Best-fitting values of the Continuum emission as a function of the orbital phase of X1822-371

Spectra	Parameters	Phase-Intervals				
		0.04-0.25	0.25-0.50	0.50-0.75	0.75-0.95	0.95-1.04
HETGS	N_H (10^{22} cm^{-2})	0.11 (fixed)	0.11 (fixed)	0.11 (fixed)	0.11 (fixed)	0.11 (fixed)
	$N_{H_{pc}}$ (10^{22} cm^{-2})	3.2 ± 0.2	3.2 ± 0.2	3.0 ± 0.2	$3.0^{+0.2}_{-0.3}$	$2.9^{+0.4}_{-0.3}$
	f	0.62 ± 0.04	0.58 ± 0.04	0.58 ± 0.05	0.60 ± 0.06	$0.60^{+0.07}_{-0.15}$
	kT$_e$ (keV)	$2.9^{+0.5}_{-0.2}$	$2.9^{+0.3}_{-0.2}$	2.6 ± 0.3	$2.8^{+0.5}_{-0.3}$	$2.8^{+1.2}_{-0.5}$
	τ	20 ± 2	20 ± 2	22 ± 2	21^{+3}_{-2}	21^{+6}_{-4}
	N_{Compst}	0.067 ± 0.009	$0.068^{+0.007}_{-0.003}$	0.054 ± 0.007	$0.050^{+0.003}_{-0.007}$	0.042 ± 0.012
	$\chi^2_{red}(d.o.f.)$	0.51(2988)	0.53(2988)	0.53(2841)	0.45(2729)	0.34(2704)
XMM	N_H (10^{22} cm^{-2})	0.10 (fixed)	0.10 (fixed)	0.10 (fixed)	0.10 (fixed)	0.10 (fixed)
	$N_{H_{pc}}$ (10^{22} cm^{-2})	$3.49^{+0.12}_{-0.14}$	3.71 ± 0.10	$3.56^{+0.05}_{-0.12}$	3.11 ± 0.14	3.7 ± 0.3
	f	0.60 ± 0.02	0.591 ± 0.014	$0.569^{+0.012}_{-0.017}$	0.58 ± 0.02	0.64 ± 0.04
	kT$_e$ (keV)	$3.07^{+0.08}_{-0.09}$	3.07 ± 0.06	3.08 ± 0.07	3.01 ± 0.08	$3.1^{+0.3}_{-0.2}$
	τ	19.7 ± 0.7	20.4 ± 0.5	$19.3^{+0.6}_{-0.5}$	21.6 ± 0.8	$18.8^{+1.6}_{-1.5}$
	N_{Compst}	$0.0407^{+0.0011}_{-0.0022}$	$0.0454^{+0.0009}_{-0.0013}$	$0.0465^{+0.0012}_{-0.0013}$	$0.0321^{+0.0006}_{-0.0013}$	$0.030^{+0.002}_{-0.004}$
	Unabs. Flux	5.92 ± 0.09	7.07 ± 0.08	6.53 ± 0.09	5.51 ± 0.09	$4.07^{+0.08}_{-0.15}$
	$\chi^2_{red}(d.o.f.)$	1.02(800)	1.05(964)	0.99(1062)	1.04(692)	0.97(457)

NOTE — Best-fitting values for the parameters of the continuum component. Uncertainties are at the 90% confidence level (hereafter c. l.) for a single parameter. The parameters are defined as in XSPEC. The equivalent hydrogen column of the local neutral matter is indicated with $N_{H_{pc}}$, the covered fraction of the emitting surface is indicated with f. The $\chi^2_{red}(d.o.f.)$ values are obtained taking into account the emission lines. The unabsorbed flux is calculated in the energy range 0.4-12 keV and it is in units of 10^{-10} erg s^{-1} cm^{-2}.

For a distance to the source of 2.5 kpc the extrapolated luminosity in the 0.1-100 keV energy range was 6×10^{35} erg s^{-1} and 1.0×10^{36} erg s^{-1} from XMM and HETGS spectra, respectively.

We performed a phase-dependent spectral analysis selecting the following five phase-intervals 0.04-0.25, 0.25-0.50, 0.50-0.75, 0.75-0.95, and 0.95-1.04, respectively. This selection allows to constrain both continuum and line emissions at different phase intervals, still having a suitable statistics to constrain the spectrum, and corresponds to the count rate rise after the eclipse, the maximum, the count rate decrease, the minimum and, finally, the eclipse, as shown in Fig. 1. We adopted the same continuum model of the averaged spectrum. Because of the lower statistics we fixed the N_H value to 0.11×10^{22} cm^{-2} and 0.10×10^{22} cm^{-2} in Chandra and XMM spectra, respectively. The electron temperature kT_e and the optical depth τ of the Comptonised component do not change along the orbit while the normalisation changes. Finally we note that the Epic-pn unabsorbed flux in the 0.4-12 keV energy range changes along the orbital period reaching the minimum during the eclipse because of the companion star occults the emitting surface, we also note that out of the eclipse the unabsorbed flux is not constant suggesting the presence of an optically thick shield that partially blocks the X-ray emission and modulates the light curve of X1822-371 with an almost sinusoidal shape (see Fig. 1).

3. Discussion

Our results are consistent with those reported by [3] using the same model to fit the continuum although we will give a different interpretation in the light of the recent works of [6] and [8] that show a large derivative of the orbital period of X1822-371. As shown in sec. 1 [8] and [6] independently concluded that X1822-371 accretes at the Eddington limit. Another clue that the luminosity of X1822-371 is at the Eddington limit is given from the ratio L_X/L_{opt}, where L_X and L_{opt} are the X-ray and optical luminosity. [10] showed that the ratio L_X/L_{opt} for X1822-371 is ~ 20, a factor 50 smaller than the typical value of 1000 for the other LMXBs. They adopted a X-ray luminosity $L_X \simeq 10^{36}$ erg s^{-1}, considering that the X-ray luminosity of X1822-371 is larger of a factor one hundred then the ratio L_X/L_{opt} is in agreement with the other LMXBs. Finally [1] showed that for a luminosity of X1822-371 at the Eddington limit The NS magnetic field assumes a conceivable value of 8×10^{10} G (see sec. 1). These four independent arguments lead us to conclude that the true luminosity of X1822-371 is at the Eddington limit.

Taking into account that the outer disc is thick and that the high inclination angle of the system is $82.5^\circ \pm 1.5^\circ$ we conclude that we are not observing the direct emission from the inner region and invoke the presence of a corona above the disc that scatters 1% of the Eddington luminosity along the line of sight, a similar scenario was discussed by [10] for this source. This scenario is different from that proposed by [3] and other authors, in fact if an extended optically thick corona is present a large part of the Eddington luminosity should be reprocessed in corona and the observed luminosity would be almost 10^{38} erg s^{-1} apart to consider the unlikely scenario in which the emission from the inner region of X1822-371 is extremely beamed.

The photons produced in the inner region near the NS are Comptonised in an optically thick plasma ($\tau \simeq 20$) with a temperature of 3 keV, the comptonising cloud is a compact region near the NS. X1822-371 has a peculiar geometry for two reasons: a) the system is observed at high inclination angle ($\sim 82^\circ.5$[4]) and b) the height H of the outer accretion disc is unusually large because the Eddington radiation from the central region illuminates the outer disc and evaporates its outer layers (see [12]). Combining these two effects we do not observe the direct emission from the central region L_0 but it is scattered by a corona. The scattered flux, considering that $\tau \ll 1$, is $L_0\left[(1-e^{-\tau})/(4\pi D^2)\right] \simeq L_0\tau/(4\pi D^2)$, where D is the distance to the source, we conclude that the scattered flux is τ times the emission produced near the NS. Assuming that $\tau \sim 0.01$ we match the expected luminosity at the Eddington limit and the observed luminosity of $\sim 10^{36}$ erg/s.

The mass function of X1822-371 is $(2.03\pm0.03)\times10^{-2}M_\odot$ ([4]), assuming a typical NS mass of $1.4M_\odot$ we derive a companion star mass of 0.408 $M_\odot$. Considering that the orbital period of X1822-371 is 5.57 hours we derive that the orbital separation is $a = 1.34\times10^{11}$ cm using the third Kepler's law. The Roche lobe of the NS and the companion star are respectively $R_{L_1} = 9.8\times10^{10}$ cm and $R_{L_2} = 3.7\times10^{10}$ cm. We obtained a mass ratio $q = M_2/M_1 \simeq 0.3$, for thie value of q the tidal truncation radius, that is the maximum possible value of the accretion disc radius R_d, is $0.43a = 5.7\times10^{10}$ cm ([5, 8]), we will adopt $R_d = 5.7\times10^{10}$ cm as outer accretion disc radius. The estimated orbital parameters allow us to infer the size of the optically thin corona assuming reasonably the Roche lobe radius R_{L_2} of the companion star is almost the radius of the companion star R_2 and taking into account the different count rates observed at mid-eclipse time and out of the eclipse. Since the spectral shape does not change along the orbit and the inclination angle

of the source is 82.5° then we impose that the change in count rates, in and out the eclipse, is mainly due to the volume of the optically thin ADC occulted by the companion star. Looking at the HETGS folded light curves of X1822-371 in Fig. 1 we observe that the count rate is $C_{ecl} \sim 3$ cts s^{-1} at the mid-eclipse time and $C_{out} \sim 6.6$ cts s^{-1} at its maximum that indicates the minimum shielding. We also note that the values of C_{ecl} and C_{out} in the EPIC-pn light curves are 37 and 84 cts s^{-1}, respectively; the results below reported are consistent considering the either the EPIC-pn or HETGS count rates. Assuming a geometry of the corona similar to that proposed by [12], where the height H of the corona increases with the distance from the neutron star ($H = kr$ with $k \leq 1$) and as maximum radius of the corona the outer accretion disc radius we derive that R_{ADC} is well constrained between 5.5 and 5.7 $\times 10^{10}$ cm depending on the height H of the ADC. We estimated that R_{ADC} is $\sim 5.5 \times 10^{10}$ cm with $R_{ADC} \simeq H$ and $R_{ADC} = R_d$ for $R_{ADC} \simeq 1.1H$. Our results imply that the corona is extended up to the outer radius of the accretion disc. In the following we assume that $R_{ADC} = R_d \sim 5.7 \times 10^{10}$ cm. Considering the ADC as an extended optically thin cloud with $\tau \sim 0.01$ we estimate that its average electron density is $n_e \sim 3 \times 10^{11}$ cm^{-3}, this value is consistent with the density of the hot corona for distance from the NS larger than 10^{10} cm ([12]).

The scenario of an extended optically thin corona is furtherly supported by the detection of the pulse period of 0.59 s in X1822-371 ([1]) that could not be detectable assuming an extended optically thick ADC because it should wash out the coherent pulsations. Our scenario predicts an extended optically thin ADC with an electron density $n_e \sim 3 \times 10^{11}$ cm^{-3} and $\tau \simeq 0.01$, the mean free path of the photons crossing the ADC is $\lambda \sim 5 \times 10^{12}$ cm, a factor 40 larger than the orbital separation of the system. We expect that only 1% of the photons is scattered in ADC, the escaping photons are scattered one time maximum and the average delay of the escaping photons is $\tau\lambda/c \simeq 2$ s. The absence of self-occultation in ADC and the spread in the arrival times of the coherent photons depends on the travelled length l in ADC. In the worst case, for the photons scattered in the outer region of the ADC $l = R_{ADC}$ then $\Delta t = R_{ADC}/c \sim 2$ s, while for the photons scattered in inner regions of the ADC, for example at $R = 10^{10}$ cm, we find $\Delta t = 0.3$ s allowing to observe the 0.59 s pulse period.

References

[1] P. G. Jonker and M. van der Klis, 2001, ApJL, 553, L43

[2] K. O. Mason and F. A. Cordova, 1982, ApJ, 255, 603

[3] R. Iaria, T. Di Salvo, L. Burderi, and N. R. Robba, 2001, ApJ, 557, 24

[4] P. G. Jonker, M. van der Klis and P. J. Groot, 2003, 339, 663

[5] J. Frank, A. King and D. Raine, 2002, *Accretion power in astrophysics*, Cambridge Univ. Press, Cambridge

[6] L. Burderi, T. di Salvo, A. Riggio, et al., A&A, 515, 44

[7] A. N. Parmar, T. Oosterbroek, S. Del Sordo, et al., 2000, A&A, 356, 175

[8] A. J. Bayless, E. L. Robinson, R. I. Hynes et al., 2010, ApJ, 709, 251

[9] N. E. White and S. S. Holt, 1982, ApJ, 257, 318

[10] C. Hellier and K. O. Mason, 1989, MNRAS, 239, 715

[11] S. Heinz S. and M. A. Nowak, 2001, MNRAS, 320, 249

[12] M. A. Jimenez-Garate, J. C. Raymond and D. A. Liedahl, 2002, ApJ, 581, 1297